

## Article

# Insights into Long-Term Acclimation Strategies of Grapevines (*Vitis vinifera* L.) in Response to Multi-Decadal Cyclical Drought

Dilrukshi S. K. Nagahatenna <sup>1,†</sup>, Tarita S. Furlan <sup>2,†</sup>, Everard J. Edwards <sup>3</sup> , Sunita A. Ramesh <sup>4</sup>   
and Vinay Pagay <sup>1,\*</sup> 

<sup>1</sup> School of Agriculture, Food and Wine, Waite Research Institute, The University of Adelaide, PMB 1, Glen Osmond, SA 5064, Australia

<sup>2</sup> Barossa Valley Estate, 9, Kraehe Rd., Marananga, SA 5355, Australia

<sup>3</sup> CSIRO Agriculture & Food, Locked Bag 2, Glen Osmond, SA 5064, Australia

<sup>4</sup> Biological Sciences, College of Science and Engineering, Flinders University, Adelaide, SA 5042, Australia

\* Correspondence: vinay.pagay@adelaide.edu.au; Tel.: +61-08-8313-0773

† These authors contributed equally to this work.

**Abstract:** Changing climatic conditions across Australia's viticulture regions is placing increasing pressure on resources such as water and energy for irrigation. Therefore, there is a pressing need to identify superior drought tolerant grapevine clones by exploring the extensive genetic diversity of early European clones in old vineyards. Previously, in a field trial, we identified drought-tolerant (DT) dry-farmed Cabernet Sauvignon clones that had higher intrinsic water use efficiency ( $WUE_i$ ) under prolonged soil moisture deficiency compared to drought-sensitive (DS) clones. To investigate whether the field-grown clones have been primed and confer the drought-tolerant phenotypes to their subsequent vegetative progenies, we evaluated the drought responses of DT and DS progenies under two sequential drought events in a glasshouse alongside progenies of commercial clones. The DT clonal progenies exhibited improved gas exchange, photosynthetic performance and  $WUE_i$  under recurrent drought events relative to DS clonal progenies. Concentration of a natural priming agent,  $\gamma$ -amino butyric acid (GABA), was significantly higher in DT progenies relative to other progenies under drought. Although DT and commercial clones displayed similar drought acclimation responses, their underlying hydraulic, stomatal and photosynthetic regulatory mechanisms were quite distinct. Our study provides fundamental insights into potential intergenerational priming mechanisms in grapevine.

**Keywords:** stress priming; leaf gas exchange; clones; water stress; water use efficiency;  $\gamma$ -amino butyric acid (GABA)



**Citation:** Nagahatenna, D.S.K.; Furlan, T.S.; Edwards, E.J.; Ramesh, S.A.; Pagay, V. Insights into Long-Term Acclimation Strategies of Grapevines (*Vitis vinifera* L.) in Response to Multi-Decadal Cyclical Drought. *Agronomy* **2022**, *12*, 3221. <https://doi.org/10.3390/agronomy12123221>

Academic Editors: Alejandro Galindo and Dugald C. Close

Received: 2 October 2022

Accepted: 10 December 2022

Published: 19 December 2022

**Publisher's Note:** MDPI stays neutral with regard to jurisdictional claims in published maps and institutional affiliations.



**Copyright:** © 2022 by the authors. Licensee MDPI, Basel, Switzerland. This article is an open access article distributed under the terms and conditions of the Creative Commons Attribution (CC BY) license (<https://creativecommons.org/licenses/by/4.0/>).

## 1. Introduction

Australia is the world's fifth-largest wine exporter [1]. The viticulture industry, which consists of wine, raisin and table grape production, is the largest fruit industry in Australia [1]. However, due to recent extreme drought events, heat waves and bushfires, Australian grapevine production reduced by 20% in 2020, and the smallest vintage was recorded: 1.4–1.5 M tons compared to the average 1.75 M tons [2]. Given that the incidence and severity of drought events are predicted to increase in the future [3], there is an increasing need to select and/or breed superior grapevine cultivars and clones, which could perform better in dry climates. Grapevine planting materials were first introduced to Australia from Europe in 1832. In the 1960s, there was a large-scale expansion of grapevine genetic resources in Australia due to the mass introduction of phylloxera-free clones with superior agronomic and oenological performance from overseas [4]. A clone is referred to as a vegetatively propagated population of vines originating from a single parent vine.

Although clonal progenies are generally considered to be genetically identical to their parent vine, over time diverse notable phenotypic variations can emerge due to progressive accumulation of spontaneous mutations [5] or epigenetic modifications [6,7]. Old Australian vineyards preserve the extensive genetic diversity of European selections, but intra-varietal genetic variability has not yet been completely explored [8]. Therefore, exploring the potential of the superior genotypes within early introductions would pave the way for improving complex traits such as drought tolerance and WUE.

Drought tolerance is a highly complex trait which is determined by genotype and environmental interactions [9–11]. Although over the past decades our knowledge on short-term drought acclimation responses has increased, a comprehensive picture of how key plant physiological processes are regulated under prolonged and cyclical drought episodes remains largely unknown [12]. The onset of water stress is marked by leaf stomatal closure. Stomatal closure is crucial in preventing excessive transpirational water loss, however, it dramatically reduces photosynthesis due to limitation in CO<sub>2</sub> influx [13]. It has long been known that stress signalling molecules such as abscisic acid (ABA) are synthesized either in root or leaf tissues under water stress conditions, and they trigger stomatal closure by triggering ion efflux and losing guard cell turgor [14–17]. Recent studies have demonstrated that aquaporin (AQP)-mediated hydraulic signals and chemical signals such as  $\gamma$ -amino butyric acid (GABA) and CLAVATA3/embryo-surrounding region-related (CLE) small peptides also contribute to long-distance communications in response to drought stress [18,19]. For instance, several studies have shown that plants accumulate  $\gamma$ -amino butyric acid (GABA), a non-protein amino acid, at the onset of the stress [20,21]. GABA is a metabolite and stress signalling molecule which is synthesized from glutamate in the cytosol [22,23] and metabolised through the GABA shunt pathway in both cytosol and mitochondria [24]. Increased concentrations of GABA under drought stress has been shown to induce stomatal closure via activation of anion channel, aluminium-activated malate transporters (ALMTs) [25]. Accumulation of GABA under stress conditions also helps activating plant's innate defence potential and pre-conditioning of the plant to next drought event through synthesising osmolytes [26], enhancing photochemical efficiency, WUE, and ROS detoxification [27–29]. Stomata progressively close as drought progresses from mild to severe stress [30]. However, when field-grown grapevines undergo severe water stress, photosynthesis is further constrained by reduction in mesophyll conductance ( $g_m$ ), biochemical limitations and reactive oxygen species (ROS)-mediated photooxidative damage [31,32].

A considerable body of evidence has recently indicated that prolonged exposure of a plant to mild to moderate biotic or abiotic stress conditions can effectively stimulate faster and stronger tolerance to subsequent stress events through the acquisition of a “stress memory” [33–35]. Priming is one of the most fascinating stress response mechanisms in plants that provides enhanced protection in a metabolically cost-effective manner without constitutively activating stress related genes [36]. To date, three types of stress memories have been identified: (1) somatic stress memory for storing information transiently for days, weeks or months within one generation; (2) intergenerational stress memory, the stress imprint that can be transmit from stressed plants only to the immediate progeny; and, (3) transgenerational stress memory, which is heritable to stress-free offspring through at least two generations (Figure 1) [37–39]. Interestingly, priming-induced “stress memory” has shown to be inherited not only through seed-derived offspring [40,41], but also to vegetatively- or asexually-propagated progenies [39]. However, the precise molecular mechanisms by which the stress imprint works in plants remains to be elucidated. Several studies have demonstrated that exposure to a priming elicitor could potentially activate sets of genes to trigger natural defense mechanisms, but the response can revert back to the pre-stress state once the priming agent is removed [36]. In contrast, epigenetic changes, which causes modification of DNA activity by methylation, histone modification or chromatin remodelling without changing the nucleotide sequence, are proposed to trigger an irreversible potent defense response for longer term protection [36,37].

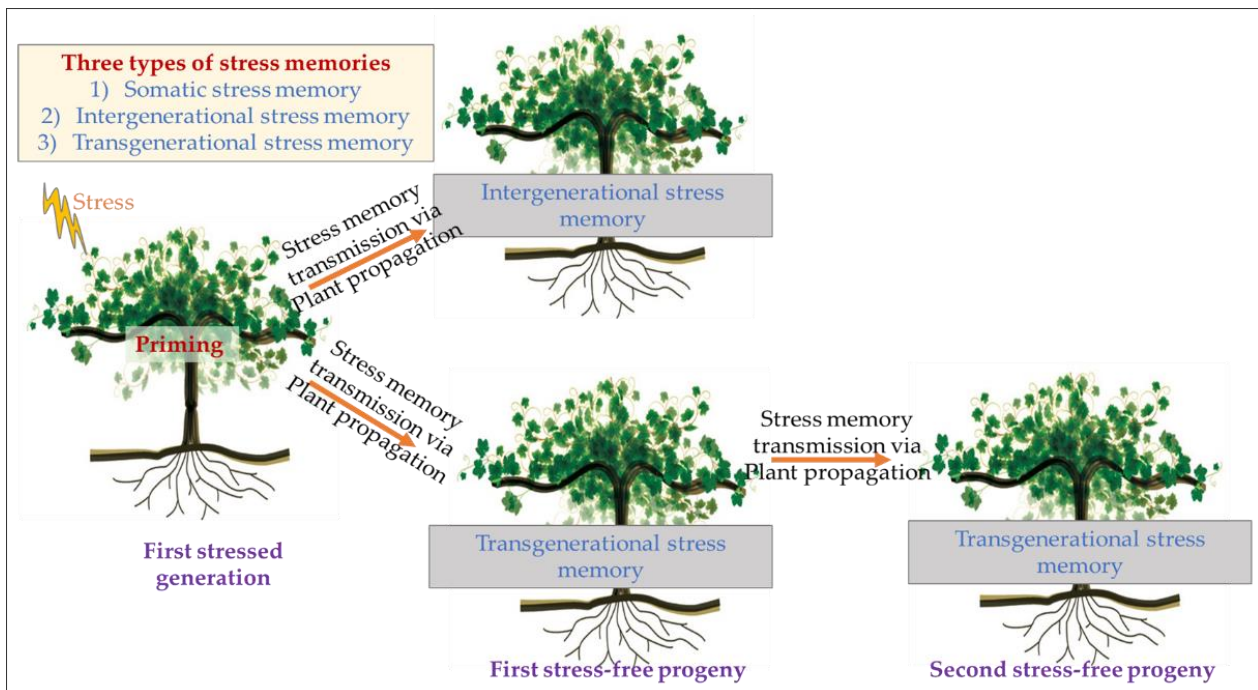


**Figure 1.** Overview of different types of stress memories in plants. Plants can be primed upon exposure to a stress event and priming enhances the plants' tolerance to severe stress conditions. Priming-associated stress memory sometimes remain only within the first stressed generation of plants (somatic stress memory). In certain circumstances, intergenerational stress memories can be transmitted to the immediate progeny whereas transgenerational memory can be passed onto many downstream progenies.

In order to understand whether woody perennial crops such as grapevine grown under multi-decadal cyclical drought have adapted to low soil moisture availability, in a previous field trial, we characterised dry-farmed Cabernet Sauvignon clones that were planted in 1954 as a mass selection of unknown clonal origin in a South Australian vineyard. Due to the extended period of dry-farming, over 65 years, these vines were ideal for unravelling long-term drought adaptation mechanisms. In our field trial, we identified several drought-tolerant (DT) clones that maintain significantly higher  $WUE_i$  under limited soil moisture compared to drought-sensitive (DS) clones [42]. We hypothesized that these superior DT clones may have been primed to water stress due to long-term exposure to limited soil moisture, and have the ability to confer the drought tolerance phenotype to their subsequent progenies via asexual propagation. In this study, we tested this hypothesis by evaluating the drought acclimation responses of DS and DT progenies under two sequential cyclic drought events in the glasshouse. To the best of our knowledge, the results obtained here are the first demonstration of intergenerational drought priming of grapevine clones.

## 2. Materials and Methods

### 2.1. Plant Materials

The drought-tolerant (DT) and drought-sensitive (DS) clones were selected based on differences in  $WUE_i$  observed under field conditions as described in our previous study [42]. Five cuttings each were vegetatively propagated from previously selected three drought-tolerant (DT) and two drought-sensitive (DS) dry-farmed clones along with three well-watered commercial clones (G9V3, CW44 and SA125) at the Yalumba Nursery (Nuriootpa, SA, Australia). Each group will be mentioned as DT, DS and commercial clonal progenies hereafter. Propagated vines were re-potted in 4.5 L pots (diameter 20 mm) with a mixture of 50% University of California soil Mix (61.5 L of sand, 38.5 L of peat moss, 50 g of calcium hydroxide, 90 g of calcium carbonate, and 100 g of Nitrophoska (12:5:1, N: P: K plus trace elements) and 50% perlite and vermiculite mix (50:50) at the Plant Research Centre (Waite Campus, University of Adelaide, Adelaide, SA, Australia). In order to facilitate similar growth rates, all vines were pruned to four nodes and incubated in a dark cool room at 4 °C for at least 25 days. All clones were grown under the glasshouse conditions with 16 h photoperiod. Two overhead supplemental light sources were turned on from 6:00 to 20:00 every day to maintain uniform light distribution and intensity ( $150 \mu\text{mol m}^{-2} \text{s}^{-1}$ ) independently of external environmental conditions. Temperature and relative humidity were continuously recorded using data loggers (Tinytag Plus 2, Gemini, Fareham, UK) in the glasshouse. After budburst, the vines were treated with 1.6 mL/L of Megamix® (13:10:15 N: P: K plus trace elements) every second week. When they reached 20-leaf stage, they were pruned to a similar leaf area.

### 2.2. Drought Cycles

In order to compare drought stress responses between DT and DS clones, 15 vines from DT clonal progeny were compared with the DS group, which consisted of 10 vines and commercial group with 15 vines. Nine vines from each DT and commercial clonal progenies and six from DS progeny were subjected to two cyclic drought events (treatment group) and remaining vines (six from DT and commercial and four from DS progenies) were included in the well-watered treatment (control group). Vines in the control group were watered daily to field capacity. Soil volumetric water content (% VWC) was measured daily using a Teros-10 soil triple sensor (METER, Pullman, WA, USA). For evaluating clonal physiological performance to drought, water was withheld from the treatment group until average soil moisture reached approx. 4% VWC. If the soil moisture dropped below 4%, the vines were watered to the equivalent pot weight until the first drought cycle (D1) was completed. They were then re-watered to field capacity and until stomatal conductance returned to similar values of the control (well-watered; Figure 2a). After full recovery from the first drought cycle, approx. 21 days after initial rewatering, a second drought cycle (D2) was imposed by withholding water as described above. Measurements and leaf tissue sampling were taken before drought stress (Day 0), at the peak of the 1st drought cycle (7 days after withholding water-D1), after full recovery from D1 (21 days after rewatering (day 0 of the second drought cycle), and at the peak of the 2nd drought cycle (4 days after withholding water-D2).

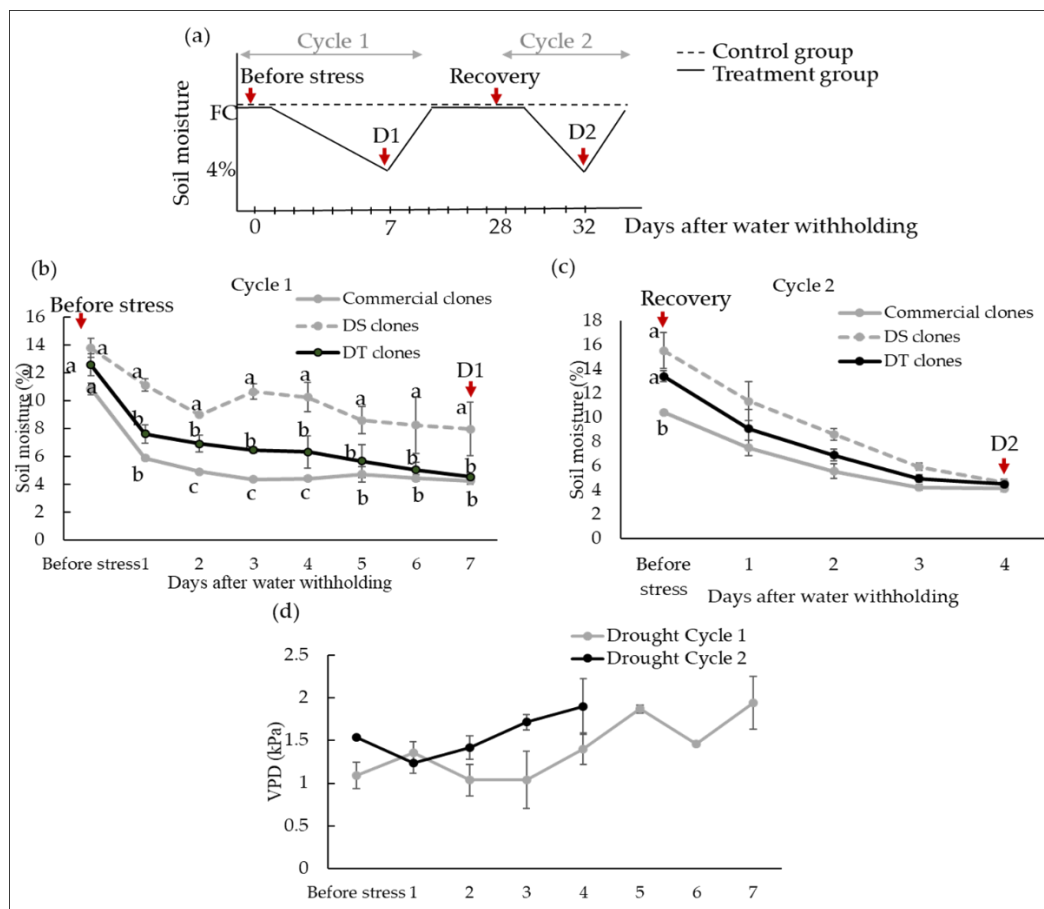


**Figure 2.** (a) Schematic representation of the experimental design: variation in soil moisture in both control (dotted lines) and treatment groups (solid lines) during two cycles of dehydration and rehydration. Arrows indicate four different time points where measurements were taken (before stress, the peak of the 1st drought cycle (D1), after full recovery, and the peak of the 2nd drought cycle (D2)). (b) Depletion of soil moisture in drought-treated commercial, DS and DT clones during 1st and (c) 2nd dehydration cycles, and (d) changes in vapour pressure deficit (VPD) during 1st (grey line) and 2nd (black line) drought events. Values are means  $\pm$  SEM of six to nine biological replicates. Statistical analysis was conducted using two-way ANOVA and lowercase letters denote statistically significant differences ( $p < 0.05$ ) between clones at each time point.

### 2.3. Midday Stem Water Potential ( $\psi_s$ ) and Leaf Gas Exchange Measurements

Midday stem water potential and in vivo gas exchange parameters were measured using a Scholander-type pressure chamber (Model 1505, PMS Instruments, Albany, NY USA) and LI-6400XT (LI-COR Inc., Lincoln, NE, USA) respectively as described in Pagay et al. (2022) [42].

### 2.4. Chlorophyll Fluorescence

Chlorophyll fluorescence parameters were measured with a LI-6400XT equipped with a leaf chamber fluorometer (model: 6400-40, LI-COR Inc., Lincoln, NE, USA) in dark- and light-adapted fully expanded leaves positioned in the bottom, middle and top levels per vine. In light-adapted leaves, the steady-state fluorescence yield ( $F_s$ ) was measured. Then, a saturating white light pulse ( $8000 \mu\text{mol m}^{-2} \text{s}^{-1}$ ) was applied for 0.8 s to achieve the light-adapted maximum fluorescence ( $F_m'$ ). The actinic light was then turned off, and far-red illumination ( $2 \mu\text{mol m}^{-2} \text{s}^{-1}$ ) was applied to measure the light-adapted initial fluorescence ( $F_0'$ ). Vines were kept overnight in darkness for dark-adapted measurements. Basal fluorescence ( $F_0$ ) and maximum fluorescence emission ( $F_m$ ) were measured by il-

luminating leaves to a weak modulating beam ( $0.03 \mu\text{mol m}^{-2} \text{s}^{-1}$ ) and a saturating white light pulse ( $8000 \mu\text{mol m}^{-2} \text{s}^{-1}$ ), respectively. Non-photochemical quenching (NPQ), photochemical quenching coefficient (qP), and actual photochemical efficiency of PSII ( $\Phi_{\text{PSII}}$ ) were calculated as:  $\text{NPQ} = (F_m - F_m')/F_m'$  [42],  $qP = (F_m' - F_s)/(F_m' - F_0')$  [43],  $\Phi_{\text{PSII}} = (F_m' - F_s)/F_m'$  [43]. Electron transport rate (ETR) was calculated according to Rahimzadeh-Bajgiran, et al. [44] using the following equations.

$$\text{ETR} = \Delta F/F_m' \times \text{PPFD} \times 0.5 \times 0.84$$

where,  $\Delta F/F_m'$  is the PSII photochemical efficiency, PPFD is the photosynthetic photon flux density incident on the leaf, 0.5 is a factor that assumes equal distribution of energy between the two photosystems, and 0.84 is the assumed leaf absorptance [45,46]. Mesophyll conductance ( $g_m$ ) was calculated using the following equation with the theoretical value of non-respiratory chloroplastic compensation point  $\Gamma^* = 42.9 \mu\text{mol mol}^{-1}$  (ppm)  $\text{CO}_2$  [47].

$$g_m = \frac{A_N}{C_i - \left[ \frac{\Gamma^*(\text{ETR} + 8(A_N + R_d))}{\text{ETR} - 4(A_N + R_d)} \right]}$$

Dark respiration ( $R_d$ ) was determined via gas exchange on dark-adapted plants (overnight at  $22^\circ\text{C}$ ).

#### 2.5. Abscisic Acid (ABA) Quantification

Approximately  $30 \mu\text{L}$  of xylem sap was extracted from leaves at the end of  $\psi_s$  measurements by increasing the balancing pressure by  $0.2\text{--}0.4 \text{ MPa}$ . Sap samples were snap frozen in liquid nitrogen and subsequently transferred to a  $-80^\circ\text{C}$  freezer until analysis. ABA abundance in xylem sap ( $\text{ABA}_{\text{xyl}}$ ) was analyzed by liquid chromatography/mass spectrometry (LC MS/MS, Agilent 6410) [11].

#### 2.6. Analysis of the Activity of Antioxidative Enzymes

In order to assess the ascorbate peroxidase (APX) enzyme activity of Cabernet clones,  $0.5 \text{ g}$  of frozen leaf samples were suspended in  $2 \text{ mL}$  of  $0.1 \text{ M}$  sodium phosphate buffer (pH 7.0) and incubated for  $10 \text{ min}$  on ice. Samples were centrifuged at  $12,000 \times g$  for  $15 \text{ min}$  and  $10 \mu\text{L}$  of the supernatant from each sample was mixed with  $290 \mu\text{L}$  of assay mixture consisting of  $0.5 \text{ mM}$  ascorbic acid,  $0.1 \text{ mM}$  EDTA- $\text{Na}_2$  and  $0.1 \text{ mM}$   $\text{H}_2\text{O}_2$  solutions prepared in  $0.05 \text{ M}$  sodium phosphate buffer (pH 7.0). The APX activity was determined by measuring the absorbance at  $290 \text{ nm}$ , in a FLUOstar Omega plate reader (BMG LABTECH GmbH, Ortenbery, Germany). The decrease in absorbance corresponded to oxidation of ascorbic acid. One enzyme unit was defined as  $1 \text{ mol}$  of ascorbic acid oxidized per minute at  $290 \text{ nm}$  [48].

#### 2.7. Quantification of GABA

GABA quantification was conducted using a GABase enzyme assay according to the protocol described in Ramesh, et al. [49]. Leaf samples were snap frozen in liquid nitrogen and  $0.1 \text{ g}$  of frozen ground samples were added to methanol and incubated at  $25^\circ\text{C}$  for  $10 \text{ min}$ . GABA was extracted from samples by vacuum drying and resuspending in  $70 \text{ mM}$   $\text{LaCl}_3$ . Samples were pelleted at  $500 \text{ g}$  in a desktop microcentrifuge, precipitated with  $1 \text{ M}$   $\text{KOH}$  and re-centrifuged at  $500 \text{ g}$ . The supernatant was used for the quantifications on an OMEGA plate-reading spectrophotometer.

#### 2.8. Gene Expression Analysis by Quantitative Real-Time PCR

Grapevine leaves that were used in  $\psi_s$  measurements were snap frozen and stored at  $-80^\circ\text{C}$  freezer. RNA was extracted using Spectrum plant total RNA kit (Sigma, Ronkonkoma, NY, USA) according to the manufacturer's instructions, and contaminated DNA was removed according to On-column DNase digestion protocol (Sigma, Ronkonkoma, NY, USA). Total RNA was quantified with a UV spectrophotometer and quality of RNA was

assessed by gel-electrophoresis. For cDNA synthesis, 1 µg of total RNA was reverse transcribed using the iScript cDNA synthesis kit (Bio-Rad, Hercules, CA, USA). In Quantitative real-time PCR (qPCR), 1 µL of 1/10 diluted cDNA was amplified in a reaction containing, 5 µL KAPA SYBR® FAST Master Mix (2X) Universal (Kapa Biosystems Inc., MA, USA), and 100 nM of gene-specific primers. qPCR primer sequences for two aquaporin (AQP) genes (*VvTIP2;1* and *VvPIP1;1*) and two stable housekeeping genes, *VvELF* and *VvUbi* were obtained from Sheldon, et al. [50]. The amplification was conducted in a QuantStudio 12K Flex Real-Time PCR system (ThermoFisher Scientific, USA) according to the following conditions: one cycle of 3 min at 95 °C followed by 40 cycles of 16 s at 95 °C, and 20 s at 60 °C. To ensure single-product amplification, melt curve analysis was performed by heating the PCR products from 60 °C to 95 °C at a ramp rate of 0.05 °C s<sup>-1</sup>. A two-round normalization of qPCR data was carried out by geometric averaging of multiple control genes as described by Vandesompele, et al. [51] and Burton, et al. [52].

### 2.9. Statistical Analysis

In order to understand the long-term drought acclimation responses of dry-farmed clones, raw data from DT, DS and commercial clonal progenies were statistically analysed using GraphPad Prism 9 software (GraphPad, San Diego, CA, USA). Due to uneven sample sizes, the two-way ANOVA was performed by fitting a mixed effects model and Tukey's multiple comparisons test. Differences were considered to be statistically significant when  $p \leq 0.05$ .

## 3. Results

### 3.1. Variations in Soil Moisture Depletion during Two Dehydration Cycles

In order to understand how dry-farmed clonal progenies perform under recurrent drought events, vegetative cuttings obtained from DT and DS clones were propagated in the glasshouse with commercial clones. Even though, propagation of both DT and commercial clonal progenies was successful, limited number of vines were obtained from DS clones. Vines in the treatment group were subjected to two recurrent drought cycles in the glasshouse (Figure 2a). Once irrigation was withheld, the soil moisture content progressively decreased to 4% VWC in all potted vines during the D1 cycle. In comparison, a steeper decline was observed during the D2 cycle (Figure 2a–c). At D1, soil moisture content decreased more rapidly in commercial clones relative to other clones, and DS clones maintained the highest soil moisture throughout this cycle (Figure 2b). However, no statistically significant differences were observed between clones during the second drought event (Figure 2c).

### 3.2. Effect of Differential Mid-Day Stem Water Potential ( $\Psi_s$ ) and Gas Exchange on Photosynthetic Performances of Dry-Farmed Clonal Progenies under Multiple Drought Events

In the control group, all irrigated clones had  $\psi_s \sim -0.4$  MPa prior to drought stress for cycle 1, but prior to cycle 2,  $\psi_s$  was significantly lower, between  $-0.6$  &  $-0.8$  MPa (Figure 3a). In drought-treated vines,  $\psi_s$  was drastically reduced to  $-1.2$  and  $-1.1$  MPa at D1 and D2, respectively, indicating a moderate to high drought stress condition, with similar  $\psi_s$  values between clones. None of the clones showed wilting symptoms or chlorosis of leaves, even under these low  $\psi_s$  values. All clones recovered after rewatering (Figure 3a).

In order to understand stomatal responses to soil drying, leaf gas exchange parameters were analysed in all clones under drought conditions. It is important to note that, well-watered vines as well as drought treated vines before commencement of the drought stress, displayed low  $g_s$  values which ranged from 0.02 to 0.08 mol H<sub>2</sub>O m<sup>-2</sup> s<sup>-1</sup> and low  $A_N$  (from 2 to 7 µmol CO<sub>2</sub> m<sup>-2</sup> s<sup>-1</sup>) irrespective of abundant soil moisture (Figure 3b,c). As those vines vigorously grew without any sign of water stress (leaf chlorosis or root growth restrictions) throughout the experiment, we speculated that low gas exchange values might be because of the low light intensities (150 µmol m<sup>-2</sup> s<sup>-1</sup>) provided during vine growth and measurements. Differences in  $g_s$  was similar between clones at D1 (Figure 3b). For

instance, when clones were exposed to the first drought event,  $g_s$  decreased in commercial, DS and DT clones by 78%, 83% and 74%, respectively compared to the clones in the control group. All clones completely recovered upon rewatering. During the second drought cycle (D2), DS clones showed further decline in  $g_s$  (93%) relative to recovery, whereas it was significantly higher in both commercial and DT clones relative to DS clones and at D1 (Figure 3b).

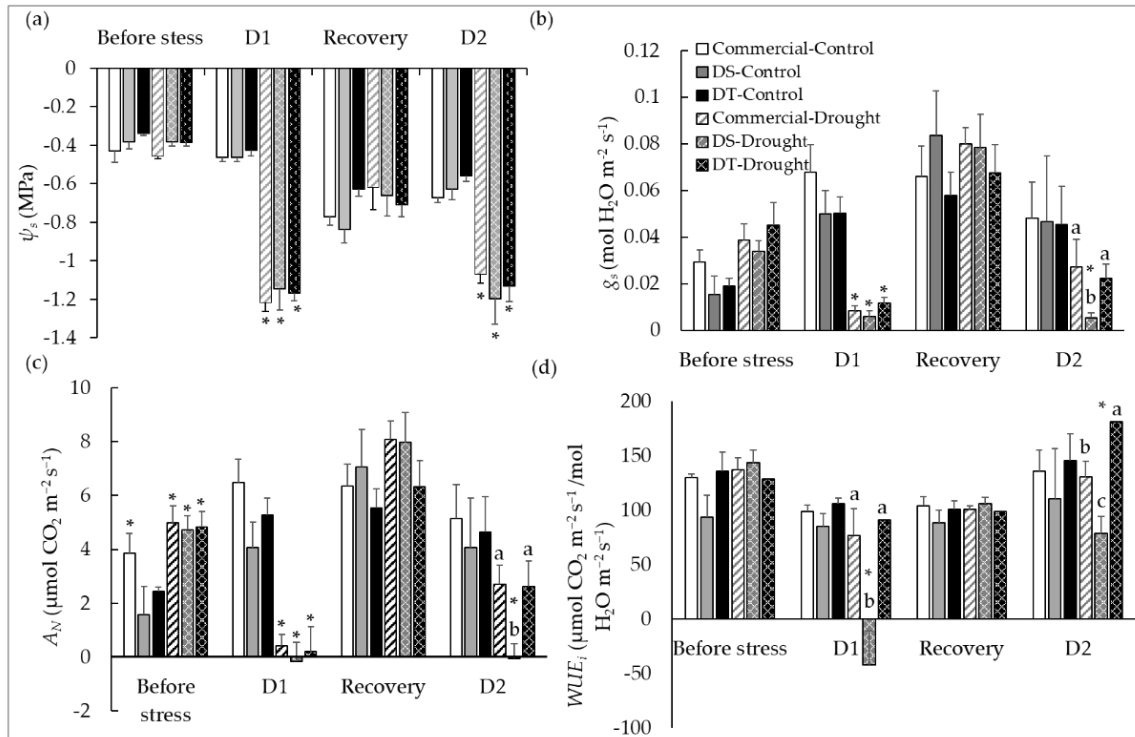


**Figure 3.** Variations in (a) mid-day stem water potential ( $\psi_s$ ), (b) stomatal conductance ( $g_s$ ), (c) net carbon assimilation ( $A_N$ ), and (d) instantaneous water use efficiency ( $WUE_i$ ) in commercial, DS and DT clones before imposition of the stress, at the first drought cycle (D1), after rewatering and at the second drought cycle (D2). Values are means  $\pm$  SEM of 4–9 biological replicates. Statistical analysis was conducted using two-way ANOVA. Asterisks indicate statistically significant differences ( $p < 0.05$ ) between drought-treated clones and controls at each treatment. Lowercase letters indicate statistically significant differences ( $p < 0.05$ ) between drought treated clones within each treatment.

Even though in the control group, all clones exhibited similar plant water status and  $g_s$ , it was consistently observed that  $A_N$  of commercial clones was significantly higher relative to other clones before drought stress was imposed. However, over time DS and DT clones also increased  $A_N$  to a similar level as commercial clones, therefore no statistical differences were apparent between clones after the start of the experiment (Figure 3c). At D1,  $A_N$  steeply decreased to near zero in all drought-stressed clones. Although  $A_N$  of DS clones was also drastically reduced to near zero at D2, in commercial and DT clones, reduction of  $A_N$  was approximately 66% and 58% respectively (Figure 3c). Leaf  $WUE_i$ , which represents the ratio of  $A_N$  versus  $g_s$ , was similar in all clones before imposing the drought stress (Figure 3d). Compared to the onset of drought stress,  $WUE_i$  at D1 was marginally reduced in commercial and DT clones by 44% and 29%, respectively, while an 83% reduction was observed in DS clones. All clones displayed basal level of  $WUE_i$  upon rewatering. When the recovered vines were exposed to the second drought event, commercial clones exhibited a 29% increase in  $WUE_i$ . However,  $WUE_i$  was marginally decreased in DS clones (26%), while, an 83% significant increase in  $WUE_i$  was observed in DT clones. DT clones exhibited significantly higher  $WUE_i$  relative to both commercial and DS clones at D2 (Figure 3d).

### 3.3. Variations in Non-Stomatal Limitations in Dry-Farmed Cabernet Clonal Progenies under Drought Stress

In comparison to the previously reported  $g_m$  values ( $0.1\text{--}0.15\text{ mol CO}_2\text{ m}^{-2}\text{ s}^{-1}$ ) in Cabernet Sauvignon [30], 68% reduction of  $g_m$  was observed in all clones at D1 but when the second drought stress was imposed, it was further reduced in both commercial and DS clones by 82% and 84%, respectively (Figure 4a). In contrast,  $g_m$  values in DT clones were significantly higher relative to the two other clones at D2 (Figure 4a). Drought stress induces changes in PSII activity and chlorophyll fluorescence traits [53]. Under non-stressed conditions, the maximum efficiency of PSII photochemistry ( $F_v/F_m$ ) and fraction of open PSII reaction centres ( $qP$ ) have reported to be around 0.75–0.80 [54,55] in Cabernet Sauvignon. Additionally, thermal dissipation of excess light energy (non-photochemical quenching; NPQ) and actual photochemical efficiency of PSII ( $\Phi_{\text{PSII}}$ ) are approximately 0.5 and 0.2, respectively [54]. In comparison to these reported values, in our study,  $F_v/F_m$  remained unchanged at 0.74–0.75 in all clones at both D1 and D2, and differences could not be detected between clones (Figure 4b). Marginal decrease in  $\Phi_{\text{PSII}}$  was observed only in DS and commercial clones upon exposure to both drought events, but in DT clones  $\Phi_{\text{PSII}}$  remained unchanged at 0.2 (Figure 4c). All clones demonstrated substantial decline in  $qP$  during both drought cycles. For instance, at D1, DS clones exhibited a marked reduction in  $qP$  (62.6%) (Figure 4d), whereas both commercial and DT clones displayed only 54.7% and 48.8% decline, respectively.  $qP$  was similar between clones at D2 (Figure 4d). During both drought cycles, NPQ was significantly higher in all clones relative to non-stressed conditions [54] (Figure 4e). During the first drought cycle, commercial clones displayed significantly higher NPQ, relative to dry-farmed clones. At the second drought stress, increase in NPQ was also observed in DS clones, however in DT clones, NPQ remained at a relatively lower level. It was interesting to note that electron transport rate (ETR) was significantly higher in DT clones relative to commercial and DS clones during both drought events (Figure 4f).

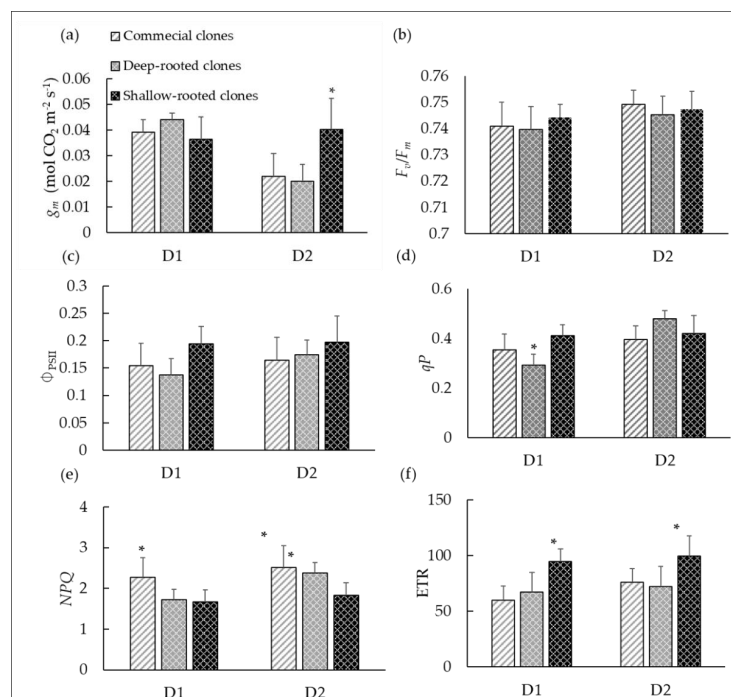


**Figure 4.** Changes in chlorophyll fluorescence parameters in dry-farmed and commercial clones at the peak of 1st and 2nd drought cycles. (a) Mesophyll conductance ( $g_m$ ), (b) maximum photochemical efficiency ( $F_v/F_m$ ), (c) actual photochemical efficiency ( $\Phi_{\text{PSII}}$ ), (d) photochemical quenching coefficient ( $qP$ ), (e) non-photochemical quenching (NPQ), and (f) electron transport rate (ETR). Values are means  $\pm$  SEM of six biological replicates. Statistical analysis was conducted using two-way ANOVA. Asterisks indicate statistically significant differences ( $p < 0.05$ ) between clones within each drought cycle.

### 3.4. Water Stress-Induced Changes in Expression of AQPs (*VvTIP2;1* and *VvPIP1;1*) in Leaves

To understand inter-clonal variation in aquaporin-mediated hydraulic regulatory mechanisms, we analysed expressions of AQP genes encoding a tonoplast intrinsic protein, *VvTIP2;1*, and a plasma membrane intrinsic protein, *VvPIP1;1* under drought stress conditions. Aquaporin transcript abundance differed significantly between clones in response to dehydration. For instance, before clones were exposed to drought stress, *VvTIP2;1* transcript abundance was significantly higher in both DS and DT clones relative to commercial clones. Irrespective of the treatment, commercial clones exhibited basal level of *VvTIP2;1* expression. However, at D1, *VvTIP2;1* expression was significantly down-regulated in both DS and DT clones and it remained constant in both clones at recovery. At D2, the transcript abundance of *VvTIP2;1* in DS clones was significantly lower relative to both commercial and DT clones (Figure 5a). *VvPIP1;1* expression was similar in all clones before exposure to drought stress whereas it was slightly down-regulated in both commercial and DT clones at D1. However, significant up-regulation of *VvPIP1;1* was observed in DS clones at D1. At the recovery stage, both commercial and DS clones displayed basal level of *VvPIP1;1* expression, but DT clones exhibited statistically non-significant increase in *VvPIP1;1* expression. At D2, *VvPIP1;1* transcript abundance was markedly increased in commercial clones. In contrast, it was decreased in both DS and DT clones at D2 (Figure 5b).

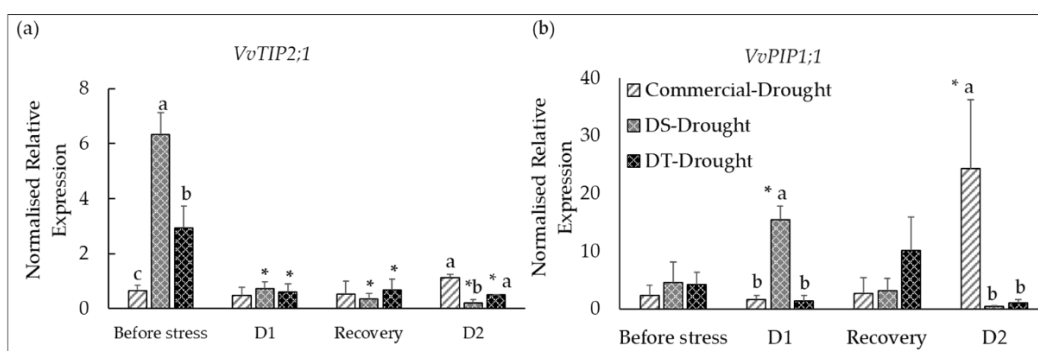


**Figure 5.** Relative gene expression (fold changes) of two aquaporin genes, (a) *VvTIP2;1* and (b) *VvPIP1;1* in Cabernet clones in response to dehydration and rehydration during two drought cycles. Values are means  $\pm$  SEM of four biological replicates. Statistical analysis was conducted using two-way ANOVA. Asterisks indicate statistically significant differences ( $p < 0.05$ ) of drought treated clones relative to before imposing the drought stress. Lowercase letters indicate statistically significant differences ( $p < 0.05$ ) between drought treated clones within each treatment.

### 3.5. Drought-Mediated Changes in ROS Detoxification

To investigate whether exposure to prolonged drought stress enhances antioxidative mechanisms in Cabernet clones, ascorbate peroxidase (APX) enzyme activity was evaluated. Interestingly, APX activity increased significantly in commercial and DS clones at D1, but it did not change in DT clones at both drought events. Upon rewatering, APX activity remained higher in commercial clones, however both DS and DT clones displayed basal level of APX activity. At the second drought event, commercial and DT clones exhibited basal level of APX enzyme activity at D2. Unfortunately, APX activity in DS clones could not be reliably detected at D2 due to sample cross-contamination (Figure 6).

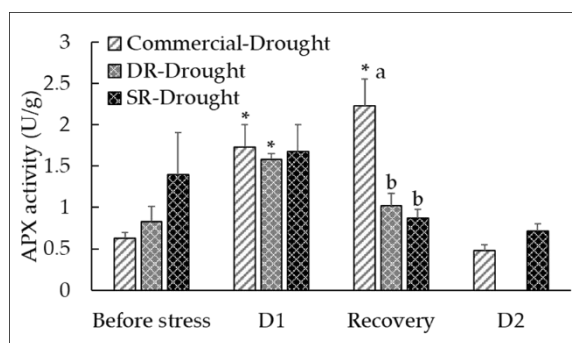


**Figure 6.** Changes in APX enzyme activity in Cabernet clones under two recurrent drought cycles. Values are means  $\pm$  SEM of six biological replicates. Statistical analysis was conducted using two-way ANOVA. Asterisks indicate statistically significant differences ( $p < 0.05$ ) of drought treated clones relative to before stress. Lowercase letters indicate statistically significant differences ( $p < 0.05$ ) between drought treated clones within each treatment.

### 3.6. Variations in ABA in the Xylem Sap ( $ABA_{xyl}$ ) and GABA Accumulation in Leaf Tissues

As large body of evidence has demonstrated that significant increase in ABA in leaves is highly correlated with the abundance of  $ABA_{xyl}$ , we investigated the drought-mediated changes in  $ABA_{xyl}$  in all Cabernet clones.  $ABA_{xyl}$  concentration increased significantly in all clones during both drought treatments and no marked differences were observed between clones. ABA levels returned to the basal levels upon rewatering (Figure 7a). Before imposition of the drought stress, similar GABA levels were detected in all three clones. Interestingly, 2-fold and 12-fold increase in GABA concentration was observed in DS and DT clones respectively at D1. However, in commercial clones, leaf GABA levels did not change in response to soil moisture content. After rewatering and at D2, basal GABA concentrations were detected in all clones (Figure 7b).

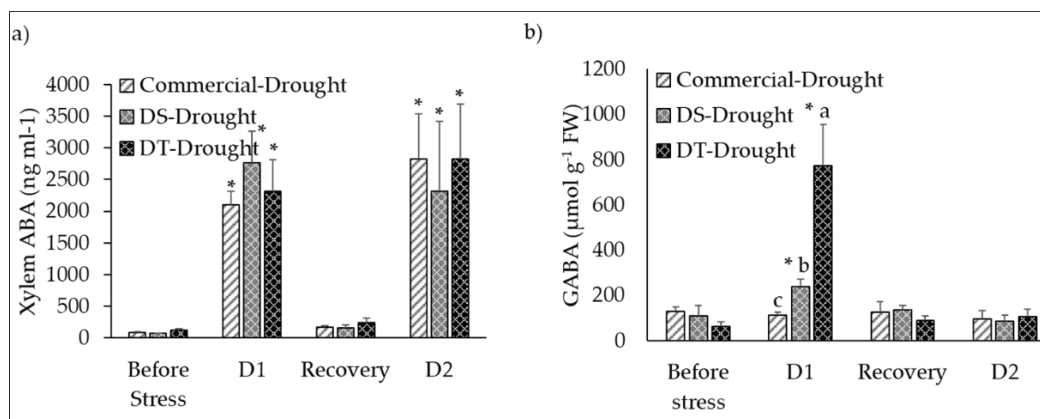


**Figure 7.** Variations in (a) ABA concentrations in the xylem sap ( $ABA_{xyl}$ ) and, (b) GABA concentrations in leaves of Cabernet clones upon exposure to two dehydration events. Values are means  $\pm$  SEM of six biological replicates. Statistical analysis was conducted using two-way ANOVA. Asterisks indicate statistically significant differences ( $p < 0.05$ ) of clones relative to well-watered conditions. Lowercase letters indicate statistically significant differences ( $p < 0.05$ ) between drought treated clones within each treatment.

## 4. Discussion

As with many commercial grapevine clones, a unique range of viticultural and oenological traits could exist between Cabernet Sauvignon dry-farmed clones used in our study due to an accumulation of somatic mutations over long period of time. However, so far, no studies have been conducted to explore the genetic variations that underlie their phenotypic differences. Previously, we reported that all superior shallow-rooted DT clones, identified

through our preliminary field trial exhibited significantly higher  $WUE_i$  under limited soil moisture relative to all selected deep-rooted DS clones grown with more soil moisture [42]. This observation tempted us to speculate that, irrespective of their potential individual genotypic and phenotypic diversity, all DT clones may have been primed in the field via a yet unexplored mechanism to become more resilient under limited soil moisture than all of the DS clones. In support of our hypothesis, Zamorano et al. (2021) [34] recently observed that the previous season’s drought stress significantly improved leaf photosynthesis rates and  $WUE_i$  in field-grown Cabernet Sauvignon under recurrent drought events. In order to test this hypothesis, all DT, DS and commercial clonal progenies were grouped separately and their physiological and molecular responses were evaluated under two recurrent cyclical drought conditions. Our study reveals that diverse drought-mediated hydraulic and stomatal regulatory mechanisms exist between Cabernet Sauvignon clones. Based on our findings, we propose simplified models which represents differential drought acclimation mechanisms in dry-farmed and commercial clones of grapevine (Figure 8).

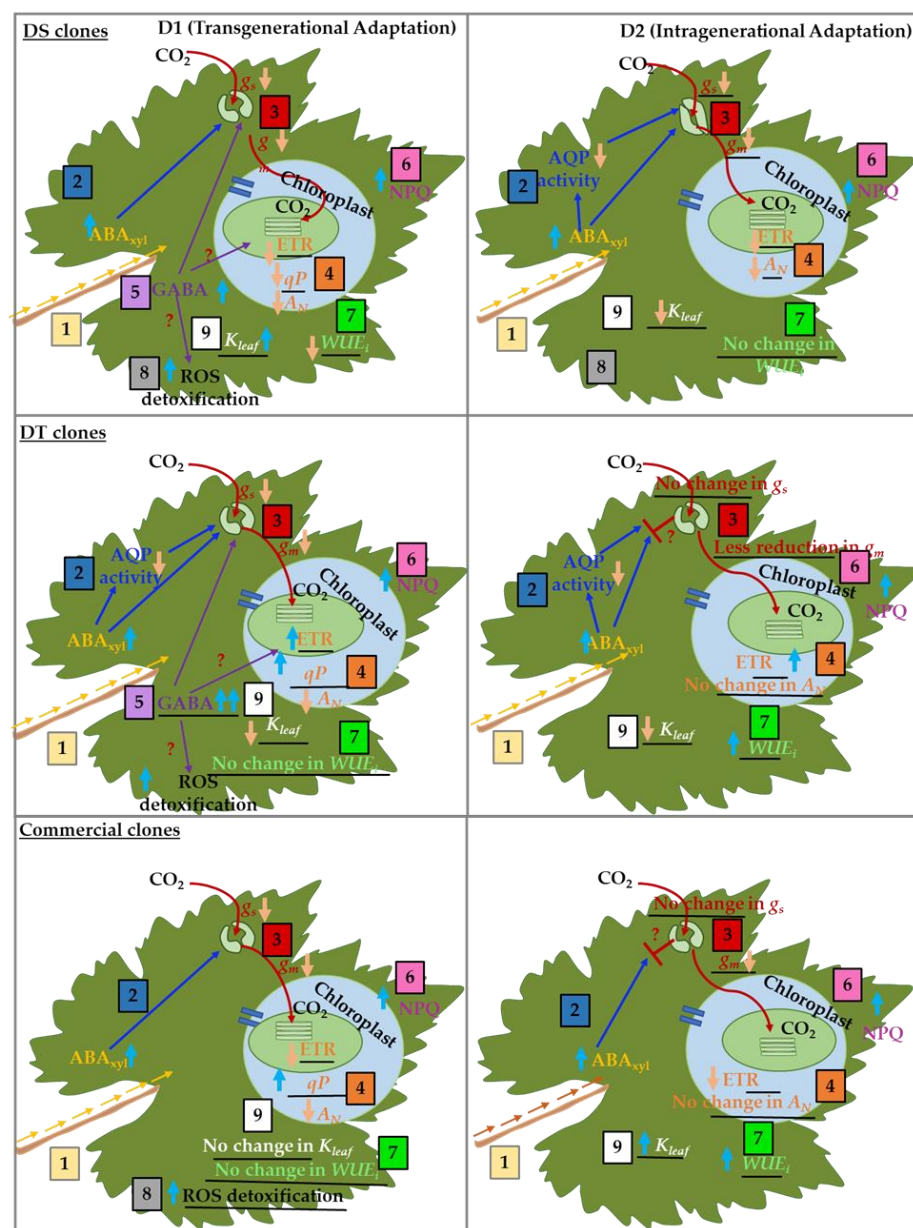


**Figure 8.** Schematic representation of differential long-term drought acclimation mechanisms of DS (top), DT (middle) and commercial (bottom) clones during first (D1; left) and second (D2; right) drought

cycles. The diagram represents (1) accumulation of  $ABA_{xy1}$  in the leaf (yellow arrows and letter), (2) ABA-dependent or ABA-AQP-mediated stomatal regulatory mechanisms (blue arrows and letter), (3)  $CO_2$  influx through stomatal and mesophyll conductance (red arrows and letters), (4) photosynthesis-associated processes (orange letters), (5) GABA-mediated priming responses (purple arrows and letters), (6) non-photochemical quenching (pink letters), (7)  $WUE_i$  (green letters), (8) antioxidative defense responses (black letters) and, (9) leaf hydraulic conductance ( $K_{leaf}$ ; white letters). Differential physiological and molecular responses observed between the clones at each drought event have been underlined. Light blue thick arrow indicates an increase or upregulation whereas orange arrow represents a decrease or downregulation. Our findings support a model in which DT clones exhibits a more efficient transgenerational drought acclimation relative to DS clones, possibly through GABA-mediated priming, improved photochemical efficiency, and  $WUE_i$  at D1. Additionally, improvement in  $CO_2$  influx through stomatal conductance, photochemical efficiency and  $WUE_i$  also contributes to stress priming of DT and commercial clones relative to DS clones at D2. Red question marks denote potential mechanisms that warrant further investigation.

#### 4.1. Differential Water Transport Capacities of Grapevine Clones under Drought Stress

During the first drought cycle, even though all clones displayed similar water flux through stomata ( $g_s$ ) and  $\psi_s$ , soil moisture content depleted more rapidly in commercial clones relative to DT and DS clones (Figures 2b and 3a,b). Given that the soil characteristics and glasshouse conditions were uniform across the experimental setting, as well as the small pots used, we assumed that the differences in soil evaporation is negligible between clones. Therefore, we speculated that significantly lower soil moisture content in commercial clones may be due to higher  $K_{leaf}$  and root water uptake capacity ( $Lp_r$ ) to facilitate higher water transport relative to DT and DS clones.

At the second drought event, all clones were able to maintain similar  $\psi_s$  irrespective of the higher evaporative demand (Figures 2c and 3a,b). However, steeper decline in soil moisture during the second drought cycle could be attributed to increased vapour pressure deficit (VPD) caused by slightly higher day/night temperature and marked reduction in relative humidity (Figure 2d, Table 1).

**Table 1.** Glasshouse environmental conditions during two drought cycles.

	Cycle 1	Cycle 2
Average Maximum Temperature (°C)	33.9	34.2
Average Minimum Temperature (°C)	12.2	12.6
Average Maximum Relative Humidity (%)	74.2	64.2
Average Minimum Relative Humidity (%)	22.5	16.8
Average Maximum VPD (kPa)	1.4	1.9
Average Minimum VPD (kPa)	1.1	1.2
Light Intensity ( $\mu\text{mol m}^{-2} \text{s}^{-1}$ )	150	150

Whole-plant water transport occurs through three routes i.e., apoplastic (through cell walls), symplastic (through plasmodesmata) and transcellular (across cell membrane) [56]. It has long been known that the AQP isoforms, which belong to the major intrinsic family (MIP), regulate transcellular or radial water transport in both leaves and roots [50,57,58]. As previous studies have shown that expressions of some Plasma membrane Intrinsic Proteins (PIPs) and Tonoplast Intrinsic Proteins (TIPs) positively correlate with  $g_s$  and  $K_{leaf}$  in grapevine [56,58,59], we tested our hypothesis by analysing expression patterns of *VvTIP2;1* and *VvPIP1;1* in grapevine leaf tissues under recurrent drought episodes.

In line with previous studies [50,59], *VvTIP2;1* expression pattern seems to have a close association with  $g_s$  under two drought events. Significant upregulation of *VvPIP1;1* was detected in DS and commercial clones at D1 and D2 respectively and DT clones exhibited statistically non-significant increase at the recovery (Figure 5a). In line with our findings,

previous studies have also shown that *VvPIP1;1* expression significantly increases [50,60] or unchanged [61] in different grapevine varieties under drought stress. Collectively, our results suggest that, at D1, AQP-mediated  $K_{leaf}$  is likely to be lower in DT clones, and higher in DS clones while commercial clones maintain constant  $K_{leaf}$ . At D2,  $K_{leaf}$  is likely to be higher in commercial clones and lower in both DT and DS clonal progenies. As AQP expression does not directly correlate with the soil drying patterns of DS and commercial clones at D1, we speculate that differences in leaf area or AQP expression in root tissues might have influenced their soil drying rates under drought stress. However, future studies are needed to confirm the exact roles of AQP in regulating  $Lp_r$  in dry-farmed grapevine clones.

As relatively isohydric varieties such as Cabernet Sauvignon are highly vulnerable to embolism, reduction of  $K_{leaf}$  has been proposed as a favourable mechanism to prevent building up the xylem tension which leads to cavitation [62,63]. Collectively, our findings suggest that DT clones may have adapted to prevent xylem embolism and consume less amount of water upon dehydration, whereas commercial clones may require relatively higher amount of water for maintaining plant metabolism under water stress.

#### 4.2. Differential Stomatal Regulatory Mechanisms Exist in Dry-Farmed and Commercial Grapevine Clones under Drought

During our experimental conditions, all clones exhibited near zero  $g_s$  at D1. During D2,  $g_s$  further declined in DS clones whereas DT and commercial clones showed significant increases (Figure 3b). In order to understand whether differential stomatal responses among clones is related to different sensitivities to key chemical and hydraulic mediators of  $g_s$ , we examined changes in concentrations of  $ABA_{xy1}$  and GABA in leaf tissues in addition to AQP expression under two drought events.

In line with previous studies [63,64],  $ABA_{xy1}$  was significantly increased in all clones during both drought events (Figure 7a). It has long been known that ABA induces stomatal closure either directly via the activation of ion channels or indirectly via restricting radial water flow from the xylem by down-regulating AQP expression [65,66]. Given the significant increase in AQP-mediated  $K_{leaf}$  and GABA concentrations in leaves, it is surmised that, at D1, stomatal closure in DS clones was induced by additive effects of chemical (ABA- and GABA-driven) mechanisms, whereas both chemical and hydraulic mechanisms are likely to exist in DT clones (Figure 8). At D2, even though both ABA- and AQP-mediated stomatal regulatory mechanisms seem to exist in both DS and DT clones, significant reduction in  $g_s$  was observed only in DS clones. Interestingly, commercial clones do not seem to have leaf hydraulic and GABA-dependent stomatal regulation under both drought events. Even though, increased accumulation of  $ABA_{xy1}$  has shown to downregulate  $g_s$  in commercial clones at D1, similar  $g_s$  reduction was not detected at D2 despite an increase in  $ABA_{xy1}$  (Figure 3b). Therefore, further investigations are required to understand whether there are other internal stimuli that prevents stomatal closure in both DT and commercial clones under recurrent drought events (Figure 8). For instance, recent work in Arabidopsis have shed light on CLAVATA3/embryo-surrounding region-related (CLE) peptides as novel messengers which are involved in root-to-shoot signalling for regulating stomatal aperture movements under drought [18,67]. However, no detailed investigations have been conducted in grapevine to understand their specific functions in stomatal regulation under long-term drought stress.

#### 4.3. Effect of Differential Hydraulic, Stomatal and Non-Stomatal Regulatory Mechanisms on Photosynthetic Performance of Dry-Farmed Clones

Our findings suggest that DT and commercial clones are able to improve plant photosynthetic performances to adapt faster to drought episodes than DS clones (Figure 3b). Overall, our results indicate that the significant decline in AN in all clones at D1 and in DS clones and D2 are likely to be associated with a decrease in  $g_s$  and  $qP$ . Interestingly, under drought stress, improved photosynthetic performances of both commercial and

DT clones can be explained as a result of improved CO<sub>2</sub> diffusion and activation of their photoprotective mechanisms.

Under steady state conditions, major metabolic processes such as photosynthesis generate highly toxic reactive oxygen species (ROS), but the potential cytotoxicity is minimized by activating ROS detoxification mechanisms. However, when plants are exposed to drought, the delicate equilibrium between ROS production and scavenging is perturbed due to limitations on CO<sub>2</sub> assimilation [68]. Different grapevine varieties possess various photoprotective mechanisms to cope with drought-mediated photoinhibition [69,70]. For instance, enhanced electron transport rate (ETR) facilitates channeling of majority of excess electrons to the photosystems [43,44]. Dissipation of excess thermal energy within chlorophyll-containing complexes via non-photochemical quenching (NPQ), also helps prevent the likelihood of formation of ROS [70]. Comprehensive studies demonstrating inter-varietal clonal differences in photo-protective mechanisms are still scarce. Our study demonstrate that such diversity is still exist between grapevine clones upon dehydration.

Previous studies have shown that APX plays a vital role in removing hydrogen peroxide (H<sub>2</sub>O<sub>2</sub>), which is the primary photosynthesis-associated ROS [71]. In line with previous studies, APX activity was significantly increased only in both commercial and DS clones at D1, but DT clones did not show increase in APX activity under both drought cycles (Figure 6). Significantly lower NPQ and higher ETR in DT clones at both drought events also imply that DT clones may have low level of acute oxidative stress relative to other clones (Figure 4e,f). As previous studies have shown that mitochondrial GABA is catabolised into succinate, which acts as an electron donor to the mitochondrial electron transport [72], we speculated that increased GABA accumulation in DT clones may help redirecting excess photochemical energy through mitochondrial electron transport system to enhance cellular respiration and therefore, DT clones may have reduced ROS-mediated photo-oxidative damage at D1 relative to both DS and commercial clones. It is interesting to further investigate whether increased electron transport in the light harvesting complex is also mediated by GABA. Even though commercial clones do not possess significant GABA-mediated ROS-detoxification mechanisms, they seemed to maintain cellular homeostasis by activating the antioxidant system and non-photochemical quenching under drought. However, increased APX activity and NPQ and low ETR in DS clones would indicate that two-fold accumulation of GABA may not be sufficient to provide complete protection against drought-induced photo-oxidative damage in DS clones (Figure 4e,f and Figure 6).

GABA is also considered an important priming agent, allowing plants to adapt faster and stronger to subsequent stress events, but, its priming-associated mechanisms are largely unknown. Given the fact that DT clones had similar level of APX activity, NPQ and ETR at both D1 and D2, we believe that GABA may play a crucial role in intergenerational priming in DT clones to enhance their long-term drought resilience. However, some fundamental questions remain unanswered. If GABA is deemed a bona fide priming elicitor, does it mediate stomatal regulation, photochemical efficiency and oxidative stress tolerance in grapevine clones (Figure 8)? Do epigenetic modifications such as DNA methylation, histone modification or chromosomal remodeling additionally contribute to intergenerational stress priming? Our ongoing work aims to further characterize drought responses of dry-farmed grapevine clones for multiple years and elucidate whether DT clones also possess transgenerational stress memory. Ultimately, the fundamental insights obtained from this study will pave the way for future research aiming towards discovering stress-memory-associated candidate genes and epigenes to develop primed-grapevine varieties for a range of changing environments particularly in the context of climate change. Additionally, this study will also be beneficial for the grapevine industry, to develop/select drought resilient genotypes and clones suitable for grapevine breeding programs.

## 5. Conclusions

The findings of our glasshouse study suggest that field-grown DT clones have a greater ability to transmit  $WUE_i$  and other drought adaptation phenotypes to their subsequent clonal progenies relative to DS clones. Although commercial clones were also found to have superior long-term drought acclimation responses similar to DT clones, our investigation found that they had distinct hydraulic, stomatal and photosynthetic mechanisms compared to the other groups. Our findings will be valuable for the clonal selection of Cabernet Sauvignon grapevines based on drought adaptation as a key trait, and pave the way for similar studies on other grapevine cultivars and crops in the future as an alternative to breeding.

**Author Contributions:** Conceptualization and design, D.S.K.N., T.S.F. and V.P.; methodology implementation, D.S.K.N., T.S.F., E.J.E. and S.A.R.; data collection and data analysis, D.S.K.N. and T.S.F.; writing original draft and editing, D.S.K.N.; review the draft, E.J.E. and V.P.; supervision, V.P. All authors have read and agreed to the published version of the manuscript.

**Funding:** No external funding was received for this work.

**Data Availability Statement:** The data presented in this study are available on request from the corresponding author.

**Acknowledgments:** The authors would like to thank Catherine M. Kidman at Wynns Coonawarra Estate and Yalumba Nursery for providing plant materials and their in-kind support, and Annette Betts (CSIRO) for assisting with the ABA analysis.

**Conflicts of Interest:** This manuscript has not been published and is not under consideration for publication elsewhere. We have no conflicts of interest to disclose and all authors have approved the manuscript and agree with its submission to the journal of MDPI Agronomy.

## References

1. Wine Australia Report. Economic Contribution of the Australian Wine Sector 2019; NSW, Australia: 2019. Available online: <https://winewa.asn.au/wp-content/uploads/2019/10/AgEconPlus-Gillespie-Economic-Contribution-Wine-Report-2019.-1-1.pdf> (accessed on 8 January 2022).
2. Wine Australia Report. National Vintage Report 2020. 2020. Available online: [https://www.wineaustralia.com/getmedia/7dcd66a7-86b5-4606-9ab7-416086077099/ML\\_VintageReport2020.pdf](https://www.wineaustralia.com/getmedia/7dcd66a7-86b5-4606-9ab7-416086077099/ML_VintageReport2020.pdf) (accessed on 8 January 2022).
3. IPCC. Climate Change 2021 the Physical Science Basis; 7 August 2021. Available online: <https://www.ipcc.ch/report/ar6/wg1> (accessed on 8 January 2022).
4. Nicholas, P. *Grapevine Clones Used in Australia*; South Australian Research and Development Institute: Adelaide, Australia, 2006.
5. Vondras, A.M.; Minio, A.; Blanco-Ulate, B.; Figueroa-Balderas, R.; Penn, M.A.; Zhou, Y.; Seymour, D.; Ye, Z.; Liang, D.; Espinoza, L.K. The genomic diversification of grapevine clones. *BMC Genom.* **2019**, *20*, 972. [[CrossRef](#)] [[PubMed](#)]
6. Xie, H.; Konate, M.; Sai, N.; Tesfamicael, K.G.; Cavagnaro, T.; Gilliham, M.; Breen, J.; Metcalfe, A.; Stephen, J.R.; De Bei, R. Global DNA methylation patterns can play a role in defining terroir in grapevine (*Vitis vinifera* cv. Shiraz). *Front. Plant Sci.* **2017**, *8*, 1860. [[CrossRef](#)] [[PubMed](#)]
7. Varela, A.; Ibañez, V.N.; Alonso, R.; Zavallo, D.; Asurmendi, S.; Talquenca, S.G.; Marfil, C.F.; Berli, F.J. Vineyard environments influence Malbec grapevine phenotypic traits and DNA methylation patterns in a clone-dependent way. *Plant Cell Rep.* **2021**, *40*, 111–125. [[CrossRef](#)]
8. Roach, M.J.; Johnson, D.L.; Bohlmann, J.; van Vuuren, H.J.; Jones, S.J.; Pretorius, I.S.; Schmidt, S.A.; Borneman, A.R. Population sequencing reveals clonal diversity and ancestral inbreeding in the grapevine cultivar Chardonnay. *PLoS Genet.* **2018**, *14*, e1007807. [[CrossRef](#)] [[PubMed](#)]
9. Lovisolo, C.; Lavoie-Lamoureux, A.; Tramontini, S.; Ferrandino, A. Grapevine adaptations to water stress: New perspectives about soil/plant interactions. *Theor. Exp. Plant Physiol.* **2016**, *28*, 53–66. [[CrossRef](#)]
10. Lovisolo, C.; Perrone, I.; Carra, A.; Ferrandino, A.; Flexas, J.; Medrano, H.; Schubert, A. Drought-induced changes in development and function of grapevine (*Vitis* spp.) organs and in their hydraulic and non-hydraulic interactions at the whole-plant level: A physiological and molecular update. *Funct. Plant Biol.* **2010**, *37*, 98–116. [[CrossRef](#)]
11. Coupel-Ledru, A.; Tyerman, S.D.; Masclef, D.; Lebon, E.; Christophe, A.; Edwards, E.J.; Simonneau, T. Abscisic acid downregulates hydraulic conductance of grapevine leaves in isohydric genotypes only. *Plant Physiol.* **2017**, *175*, 1121–1134. [[CrossRef](#)]
12. Seleiman, M.F.; Al-Suhaibani, N.; Ali, N.; Akmal, M.; Alotaibi, M.; Refay, Y.; Dindaroglu, T.; Abdul-Wajid, H.H.; Battaglia, M.L. Drought stress impacts on plants and different approaches to alleviate its adverse effects. *Plants* **2021**, *10*, 259. [[CrossRef](#)]
13. Chaves, M.M. Effects of water deficits on carbon assimilation. *J. Exp. Bot.* **1991**, *42*, 1–16. [[CrossRef](#)]

14. Yoshida, R.; Umezawa, T.; Mizoguchi, T.; Takahashi, S.; Takahashi, F.; Shinozaki, K. The regulatory domain of SRK2E/OST1/SnRK2.6 interacts with ABI1 and integrates abscisic acid (ABA) and osmotic stress signals controlling stomatal closure in Arabidopsis. *J. Biol. Chem.* **2006**, *281*, 5310–5318. [[CrossRef](#)]
15. Rossdeutsch, L.; Edwards, E.; Cookson, S.J.; Barrieu, F.; Gambetta, G.A.; Delrot, S.; Ollat, N. ABA-mediated responses to water deficit separate grapevine genotypes by their genetic background. *BMC Plant Biol.* **2016**, *16*, 91. [[CrossRef](#)] [[PubMed](#)]
16. Joshi-Saha, A.; Valon, C.; Leung, J. Abscisic acid signal off the STARting block. *Mol. Plant* **2011**, *4*, 562–580. [[CrossRef](#)] [[PubMed](#)]
17. Kim, T.-H.; Böhmer, M.; Hu, H.; Nishimura, N.; Schroeder, J.I. Guard cell signal transduction network: Advances in understanding abscisic acid, CO<sub>2</sub>, and Ca<sup>2+</sup> signaling. *Annu. Rev. Plant Biol.* **2010**, *61*, 561–591. [[CrossRef](#)] [[PubMed](#)]
18. Takahashi, F.; Suzuki, T.; Osakabe, Y.; Betsuyaku, S.; Kondo, Y.; Dohmae, N.; Fukuda, H.; Yamaguchi-Shinozaki, K.; Shinozaki, K. A small peptide modulates stomatal control via abscisic acid in long-distance signalling. *Nature* **2018**, *556*, 235–238. [[CrossRef](#)]
19. Christmann, A.; Grill, E. Peptide signal alerts plants to drought. *Nature* **2018**, *556*, 178–179. [[CrossRef](#)]
20. Ramesh, S.A.; Tyerman, S.D.; Xu, B.; Bose, J.; Kaur, S.; Conn, V.; Domingos, P.; Ullah, S.; Wege, S.; Shabala, S. GABA signalling modulates plant growth by directly regulating the activity of plant-specific anion transporters. *Nat. Commun.* **2015**, *6*, 7879. [[CrossRef](#)]
21. Vijayakumari, K.; Puthur, J.T.  $\gamma$ -Aminobutyric acid (GABA) priming enhances the osmotic stress tolerance in *Piper nigrum* Linn. plants subjected to PEG-induced stress. *Plant Growth Regul.* **2016**, *78*, 57–67. [[CrossRef](#)]
22. Bouché, N.; Lacombe, B.T.; Fromm, H. GABA signaling: A conserved and ubiquitous mechanism. *Trends Cell Biol.* **2003**, *13*, 607–610. [[CrossRef](#)]
23. Bown, A.W.; Shelp, B.J. Plant GABA: Not Just a Metabolite. *Trends Plant Sci.* **2016**, *21*, 811–813. [[CrossRef](#)]
24. Michaeli, S.; Fromm, H. Closing the loop on the GABA shunt in plants: Are GABA metabolism and signaling entwined? *Front. Plant Sci.* **2015**, *6*, 419. [[CrossRef](#)]
25. Xu, B.; Long, Y.; Feng, X.; Zhu, X.; Sai, N.; Chirkova, L.; Betts, A.; Herrmann, J.; Edwards, E.J.; Okamoto, M. GABA signalling modulates stomatal opening to enhance plant water use efficiency and drought resilience. *Nat. Commun.* **2021**, *12*, 11952. [[CrossRef](#)]
26. Shelp, B.J.; Bown, A.W.; McLean, M.D. Metabolism and functions of gamma-aminobutyric acid. *Trends Plant Sci.* **1999**, *4*, 446–452. [[CrossRef](#)] [[PubMed](#)]
27. Krishnan, S.; Laskowski, K.; Shukla, V.; Merewitz, E.B. Mitigation of drought stress damage by exogenous application of a non-protein amino acid  $\gamma$ -aminobutyric acid on perennial ryegrass. *J. Am. Soc. Hortic. Sci.* **2013**, *138*, 358–366. [[CrossRef](#)]
28. Nayyar, H.; Kaur, R.; Kaur, S.; Singh, R.  $\gamma$ -Aminobutyric acid (GABA) imparts partial protection from heat stress injury to rice seedlings by improving leaf turgor and upregulating osmoprotectants and antioxidants. *J. Plant Growth Regul.* **2014**, *33*, 408–419. [[CrossRef](#)]
29. Yang, A.; Cao, S.; Yang, Z.; Cai, Y.; Zheng, Y.  $\gamma$ -Aminobutyric acid treatment reduces chilling injury and activates the defence response of peach fruit. *Food Chem.* **2011**, *129*, 1619–1622. [[CrossRef](#)]
30. Medrano, H.; Escalona, J.M.; Bota, J.; Gulias, J.; Flexas, J. Regulation of photosynthesis of C3 plants in response to progressive drought: Stomatal conductance as a reference parameter. *Ann. Bot.* **2002**, *89*, 895–905. [[CrossRef](#)] [[PubMed](#)]
31. Tomás, M.; Medrano, H.; Brugnoli, E.; Escalona, J.M.; Martorell, S.; Pou, A.; Ribas-Carbó, M.; Flexas, J. Variability of mesophyll conductance in grapevine cultivars under water stress conditions in relation to leaf anatomy and water use efficiency. *Aust. J. Grape Wine Res.* **2014**, *20*, 272–280. [[CrossRef](#)]
32. Flexas, J.; Galmes, J.; Galle, A.; Gulias, J.; Pou, A.; Ribas-Carbo, M.; Tomas, M.; Medrano, H. Improving water use efficiency in grapevines: Potential physiological targets for biotechnological improvement. *Aust. J. Grape Wine Res.* **2010**, *16*, 106–121. [[CrossRef](#)]
33. Alves, R.D.; Menezes-Silva, P.E.; Sousa, L.F.; Loram-Lourenço, L.; Silva, M.L.; Almeida, S.E.; Silva, F.G.; de Souza, L.P.; Fernie, A.R.; Farnese, F.S. Evidence of drought memory in *Diptery × alata* indicates differential acclimation of plants to savanna conditions. *Sci. Rep.* **2020**, *10*, 16455. [[CrossRef](#)]
34. Zamorano, D.; Franck, N.; Pastenes, C.; Wallberg, B.; Garrido, M.; Silva, H. Improved physiological performance in grapevine (*Vitis vinifera* L.) cv. Cabernet Sauvignon facing recurrent drought stress. *Aust. J. Grape Wine Res.* **2021**, *27*, 258–268. [[CrossRef](#)]
35. Tombesi, S.; Frioni, T.; Poni, S.; Palliotti, A. Effect of water stress “memory” on plant behavior during subsequent drought stress. *Environ. Exp. Bot.* **2018**, *150*, 106–114. [[CrossRef](#)]
36. Bruce, T.J.A.; Matthes, M.C.; Napier, J.A.; Pickett, J.A. Stressful “memories” of plants: Evidence and possible mechanisms. *Plant Sci.* **2007**, *173*, 603–608. [[CrossRef](#)]
37. Lämke, J.; Bäurle, I. Epigenetic and chromatin-based mechanisms in environmental stress adaptation and stress memory in plants. *Genome Biol.* **2017**, *18*, 124. [[CrossRef](#)] [[PubMed](#)]
38. Hilker, M.; Schmölling, T. Stress priming, memory, and signalling in plants. *Plant Cell Environ.* **2019**, *42*, 753–761. [[CrossRef](#)] [[PubMed](#)]
39. Jacques, C.; Salon, C.; Barnard, R.L.; Vernoud, V.; Prudent, M. Drought stress memory at the plant cycle level: A review. *Plants* **2021**, *10*, 1873. [[CrossRef](#)]
40. Springer, N.M.; Schmitz, R.J. Exploiting induced and natural epigenetic variation for crop improvement. *Nat. Rev. Genet.* **2017**, *18*, 563–575. [[CrossRef](#)]

41. Hagemann, J.; Becker, C.; Muller, J.; Stegle, O.; Meyer, R.C.; Wang, G.; Schneeberger, K.; Fitz, J.; Altmann, T.; Bergelson, J.; et al. Century-scale methylome stability in a recently diverged *Arabidopsis thaliana* lineage. *PLoS Genet.* **2015**, *11*, e1004920. [[CrossRef](#)]
42. Pagay, V.; Furlan, T.S.; Kidman, C.M.; Nagahatenna, D. Long-term drought adaptation of unirrigated grapevines (*Vitis vinifera* L.). *Theor. Exp. Plant Physiol.* **2022**, *34*, 215–225. [[CrossRef](#)]
43. Murchie, E.H.; Lawson, T. Chlorophyll fluorescence analysis: A guide to good practice and understanding some new applications. *J. Exp. Bot.* **2013**, *64*, 3983–3998. [[CrossRef](#)]
44. Rahimzadeh-Bajgiran, P.; Tubuxin, B.; Omasa, K. Estimating chlorophyll fluorescence parameters using the joint Fraunhofer Line depth and laser-induced saturation pulse (FLD-LISP) method in different plant species. *Remote Sens.* **2017**, *9*, 599. [[CrossRef](#)]
45. Flexas, J.; Escalona, J.; Medrano, H. Down-regulation of photosynthesis by drought under field conditions in grapevine leaves. *Funct. Plant Biol.* **1998**, *25*, 893–900. [[CrossRef](#)]
46. Maxwell, K.; Johnson, G.N. Chlorophyll fluorescence—A practical guide. *J. Exp. Bot.* **2000**, *51*, 659–668. [[CrossRef](#)] [[PubMed](#)]
47. Galle, A.; Florez-Sarasa, I.; Thameur, A.; de Paepe, R.; Flexas, J.; Ribas-Carbo, M. Effects of drought stress and subsequent rewatering on photosynthetic and respiratory pathways in *Nicotiana sylvestris* wild type and the mitochondrial complex I-deficient CMSII mutant. *J. Exp. Bot.* **2010**, *61*, 765–775. [[CrossRef](#)] [[PubMed](#)]
48. Sun, J.; You, X.; Li, L.; Peng, H.; Su, W.; Li, C.; He, Q.; Liao, F. Effects of a phospholipase D inhibitor on postharvest enzymatic browning and oxidative stress of litchi fruit. *Postharvest Biol. Technol.* **2011**, *62*, 288–294. [[CrossRef](#)]
49. Ramesh, S.A.; Kamran, M.; Sullivan, W.; Chirkova, L.; Okamoto, M.; Degryse, F.; McLaughlin, M.; Gilliam, M.; Tyerman, S.D. Aluminum-activated malate transporters can facilitate GABA transport. *Plant Cell* **2018**, *30*, 1147–1164. [[CrossRef](#)]
50. Shelden, M.C.; Vandeleur, R.; Kaiser, B.N.; Tyerman, S.D. A comparison of petiole hydraulics and aquaporin expression in an anisohydric and isohydric cultivar of grapevine in response to water-stress induced cavitation. *Front. Plant Sci.* **2017**, *8*, 1893. [[CrossRef](#)]
51. Vandesompele, J.; De Preter, K.; Pattyn, F.; Poppe, B.; Van Roy, N.; De Paepe, A.; Speleman, F. Accurate normalization of real-time quantitative RT-PCR data by geometric averaging of multiple internal control genes. *Genome Biol.* **2002**, *3*, research0034.1. [[CrossRef](#)]
52. Burton, R.A.; Shirley, N.J.; King, B.J.; Harvey, A.J.; Fincher, G.B. The CesA gene family of barley. Quantitative analysis of transcripts reveals two groups of co-expressed genes. *Plant Physiol.* **2004**, *134*, 224–236. [[CrossRef](#)]
53. Menezes-Silva, P.E.; Sanglard, L.; Avila, R.T.; Morais, L.E.; Martins, S.C.V.; Nobres, P.; Patreze, C.M.; Ferreira, M.A.; Araujo, W.L.; Fernie, A.R.; et al. Photosynthetic and metabolic acclimation to repeated drought events play key roles in drought tolerance in coffee. *J. Exp. Bot.* **2017**, *68*, 4309–4322. [[CrossRef](#)]
54. Guan, X.; Gu, S. Photorespiration and photoprotection of grapevine (*Vitis vinifera* L. cv. Cabernet Sauvignon) under water stress. *Photosynthetica* **2009**, *49*, 437–444. [[CrossRef](#)]
55. Min, Z.; Li, R.; Chen, L.; Zhang, Y.; Li, Z.; Liu, M.; Ju, Y.; Fang, Y. Alleviation of drought stress in grapevine by foliar-applied strigolactones. *Plant Physiol. Biochem.* **2019**, *135*, 99–110. [[CrossRef](#)]
56. Maurel, C.; Simonneau, T.; Sutka, M. The significance of roots as hydraulic rheostats. *J. Exp. Bot.* **2010**, *61*, 3191–3198. [[CrossRef](#)]
57. Vandeleur, R.K.; Sullivan, W.; Athman, A.; Jordans, C.; Gilliam, M.; Kaiser, B.N.; Tyerman, S.D. Rapid shoot-to-root signalling regulates root hydraulic conductance via aquaporins. *Plant Cell Environ.* **2014**, *37*, 520–538. [[CrossRef](#)]
58. Shelden, M.C.; Howitt, S.M.; Kaiser, B.N.; Tyerman, S.D. Identification and functional characterisation of aquaporins in the grapevine, *Vitis vinifera*. *Funct. Plant Biol.* **2009**, *36*, 1065–1078. [[CrossRef](#)]
59. Sabir, F.; Zarrouk, O.; Noronha, H.; Loureiro-Dias, M.C.; Soveral, G.; Gerós, H.; Prista, C. Grapevine aquaporins: Diversity, cellular functions, and ecophysiological perspectives. *Biochimie* **2021**, *188*, 61–76. [[CrossRef](#)]
60. Dayer, S.; Scharwies, J.D.; Ramesh, S.A.; Sullivan, W.; Doerflinger, F.C.; Pagay, V.; Tyerman, S.D. Comparing hydraulics between two grapevine cultivars reveals differences in stomatal regulation under water stress and exogenous ABA applications. *Front. Plant Sci.* **2020**, *11*, 705. [[CrossRef](#)]
61. Pou, A.; Medrano, H.; Flexas, J.; Tyerman, S.D. A putative role for TIP and PIP aquaporins in dynamics of leaf hydraulic and stomatal conductances in grapevine under water stress and re-watering. *Plant Cell Environ.* **2013**, *36*, 828–843. [[CrossRef](#)] [[PubMed](#)]
62. Schultz, H.R. Differences in hydraulic architecture account for near-isohydric and anisohydric behaviour of two field-grown *Vitis vinifera* L. cultivars during drought. *Plant Cell Environ.* **2003**, *26*, 1393–1405. [[CrossRef](#)]
63. Gerzon, E.; Biton, I.; Yaniv, Y.; Zemach, H.; Netzer, Y.; Schwartz, A.; Fait, A.; Ben-Ari, G. Grapevine Anatomy as a Possible Determinant of Isohydric or Anisohydric Behavior. *Am. J. Enol. Vitic.* **2015**, *66*, 340–347. [[CrossRef](#)]
64. Bano, A.; Dorffling, K.; Bettin, D.; Hahn, H. Abscisic acid and cytokinins as possible root-to-shoot signals in xylem sap of rice plants in drying soil. *Funct. Plant Biol.* **1993**, *20*, 109–115. [[CrossRef](#)]
65. Munns, R.; Cramer, G. Is coordination of leaf and root growth mediated by abscisic acid? Opinion. *Plant Soil* **1996**, *185*, 33–49. [[CrossRef](#)]
66. Shatil-Cohen, A.; Attia, Z.; Moshelion, M. Bundle-sheath cell regulation of xylem-mesophyll water transport via aquaporins under drought stress: A target of xylem-borne ABA? *Plant J.* **2011**, *67*, 72–80. [[CrossRef](#)] [[PubMed](#)]
67. Fletcher, J.C. Recent advances in *Arabidopsis* CLE peptide signaling. *Trends Plant Sci.* **2020**, *25*, 1005–1016. [[CrossRef](#)] [[PubMed](#)]
68. Cruz de Carvalho, M.H. Drought stress and reactive oxygen species: Production, scavenging and signaling. *Plant Signal. Behav.* **2008**, *3*, 156–165. [[CrossRef](#)] [[PubMed](#)]

69. Hochberg, U.; Degu, A.; Fait, A.; Rachmilevitch, S. Near isohydric grapevine cultivar displays higher photosynthetic efficiency and photorespiration rates under drought stress as compared with near anisohydric grapevine cultivar. *Physiol. Plant.* **2013**, *147*, 443–452. [[CrossRef](#)] [[PubMed](#)]
70. Guan, X.; Zhao, S.; Li, D.; Shu, H. Photoprotective function of photorespiration in several grapevine cultivars under drought stress. *Photosynthetica* **2004**, *42*, 31–36. [[CrossRef](#)]
71. Roach, T.; Krieger-Liszkay, A. Regulation of photosynthetic electron transport and photoinhibition. *Curr. Protein Pept. Sci.* **2014**, *15*, 351–362. [[CrossRef](#)]
72. Foyer, C.H.; Noctor, G. Redox sensing and signalling associated with reactive oxygen in chloroplasts, peroxisomes and mitochondria. *Physiol. Plant.* **2003**, *119*, 355–364. [[CrossRef](#)]